

P. Placke
V. Edel
L. Reversat
R. Richert
E.W. Fischer

Field-induced structural ordering in electrorheological fluids

Received: 2 June 1995
Accepted: 23 August 1995

P. Placke · V. Edel · L. Reversat
R. Richert (✉) · E.W. Fischer
Max-Planck-Institut für Polymerforschung
Ackermannweg 10
55128 Mainz, Germany

Abstract Structural relaxations of an electrorheological fluid (ERF) due to changes in the applied electrical field strength or shear rate are observed on time scales $1\text{ s} < t < 40\,000\text{ s}$. Commercial ERFs consisting of mesoscopic polyurethane particles in a silicone oil matrix were studied by three different experimental techniques in order to obtain and compare the characteristic relaxation times. It is demonstrated that dielectric spectroscopy, viscosimetry and light transmission experiments represent the same results concerning the structural relaxation phenomena of ERFs when electrical fields are applied. The tendency of strong

induced dipoles to align the particles in the direction of the field increases the effective dipole moment and therefore $\Delta\epsilon$, the shear viscosity η and the amount of light transmitted along the field direction in an ITO/glass sandwich cell. The optical experiment is capable of resolving fast processes within the first 1 ms if large electrical fields are applied. The effects of electrophoresis and shearing, which both counteract the field induced structures, are also addressed.

Key words Electrorheological fluids – colloids – rheodielectric spectroscopy – light transmission

Introduction

Many research activities regarding ERFs describe the impact of an electrical field and of the composition on the viscosity, while more recent investigations focus on the time dependence of structure formation in the time regime 0.1 ms to 10 s [1–3]. In the present work the dynamics of structure formation as a function of electric field or shear rate are investigated by dielectric spectroscopy, rheology and light transmission experiments for extended time ranges. The link between rheological properties of the ERF and its dielectric constants or light transmission coefficients bases on structure formation of particles affecting the viscosity, optical transmission and correlations among the dipoles which alter the effective dipole moments and thus the dielectric constant [4–9]. The basis for

this structure formation relies on the heterogeneity of the fluid, composed of electrically conducting particles (filler) suspended in a more insulating oil matrix. An external electrical field applied to such systems induces strong electric dipoles within the particles known as Maxwell–Wagner polarization [9], which gives rise to substantial electrostatic interactions. Here we focus on low electrical field strength, below those applied in technical applications, and on relatively small values for the shear rate, where particle rotation does not counteract their electrical polarization.

The stability of sample properties like dielectric constant, viscosity or transmission is observed in long time experiments ($0.5\text{ s} < t < 40\,000\text{ s}$) for a commercial ERF [10, 11]. As addressed in more detail in an earlier paper [12], we quantify the structural changes by an index K , which relates to an observable, $\Delta\epsilon$, σ_M , or I , normalized to

its value in the case $E = 0$ or $\dot{\gamma} = 0$. We find the initial change of these properties being destroyed by a variety of slow relaxation phenomena, which arise from electrophoresis or movements of large particle agglomerates on time scales $t > 10$ s. They are strongly dependent on factors like constant or alternating electrical bias field, shear rate, and temperature. Additionally, the phenomena after the removal of an electrical field are observed. In some cases the relaxation of the ERF to the initial state takes several hours. These present studies extend our previous [12] work in this field.

Experiment

Sample properties

The commercial electrorheological fluid studied here (Rheobay TP AI 3565, Bayer) [10, 11] consists of polyurethane particles in a silicone oil matrix. The average particle diameter is $d = 5 \mu\text{m}$, their volume fraction in the liquid is about 60%. Salt is added in order to achieve a sufficient conductivity within the particles such that dipoles can be induced by an external electrical field. Before starting an experiment the samples are mixed for several hours and exposed to an ultrasonic bath in order to destroy possible aggregates and to reduce sedimentation of the particles.

Experimental setup

The rheodielectric apparatus combines two independent systems [12]. One is a Bohlin VOR rheometer with its control unit and the second is a dielectric spectroscopy setup with a personal computer acquiring the data and controlling the entire experiment. We had to modify the rheometers Couette cell consisting of two concentric cylinders (bob and cup) with insulation in order to enable the simultaneous dielectric experiments. The gap between bob ($\varnothing = 14$ mm) and cup is $400 \mu\text{m}$, $650 \mu\text{m}$ or 1 mm. We designed a special AC/DC-crossway to avoid damage to the LCR-meter HP 4284A caused by high dc-voltages. This setup enables viscosimetric experiments in the shear rate regime from 0 to 1600 s^{-1} and dielectric spectroscopy for frequencies ranging from 100 Hz to 1 MHz where additional electrical bias fields (0 ± 625 V/mm) can be applied, either with constant or alternating (0.75 Hz) polarity. The time-dependent measurements were recorded at fixed dielectric frequencies (harmonic field with $f = 1$ kHz or 4 kHz).

The experimental setup for light transmission studies is presented in Fig. 1. A He-Ne-laser beam ($\lambda = 633$ nm) illu-

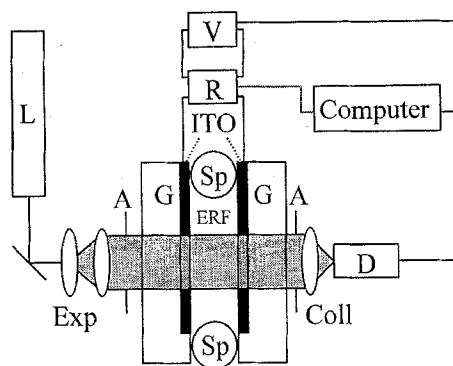


Fig. 1 Schematic setup of the light transmission experiment. L: He-Ne-Laser (10 mW), EXP: beam expander, Coll: collimator, A: aperture, V: dc-supply, R: switch box, D: photo-diode, G: glass plates, SP: spacer $150 \mu\text{m}$, ITO: Indium-Tin-oxide electrodes, ERF: Electrorheological fluid

minates the sample which is sandwiched between two transparent glass plates with ITO-electrodes. The electrodes are spaced about $150 \mu\text{m}$, so that electrical fields ranging from 0 to 1300 V/mm can be applied. The laser light transmitting the cell parallel to the direction of the electrical field is detected by a photo-diode (Siemens BPW-34), while the signal of the diode is measured by an AD conversion card (Keithley Metrabyte DAS-801). This setup allows to monitor the reaction of the ERF due to changes in the applied electrical field strength with a time resolution better than 1 ms. Shearing the sample in this cell is impossible.

Results

Dielectric spectra for different electrical field strengths ($0 < E < 400$ V/mm) were fitted by using a Cole-Cole function [9] with an additional conductivity term, which yield the characteristic values relaxation strength $\Delta\epsilon$, relaxation time τ_D and dc-conductivity σ_{dc} . For an experiment where the field is applied 3 min prior to each measurement, Fig. 2 indicates a strong increase of σ_{dc} as the field exceeds ≈ 250 V/mm. Before measuring the dielectric and mechanical properties of the ERFs, the pure matrix, silicone oil, has been investigated with the result that no significant changes in the dielectric and mechanical properties are observed when applying large electrical fields. The relaxation strength $\Delta\epsilon$ of the ERF as obtained from dielectric data $\epsilon^*(\omega)$ [12] stems from the Maxwell-Wagner polarization (MWP) [9, 12] and decreases for $E \geq 250$ V/mm (see Fig. 2), probably as a direct consequence of the observed $\sigma_{dc}(E)$ in Fig. 2, because the conductivities of particles and matrix become more similar in the high field regime. Independent of the reason for the

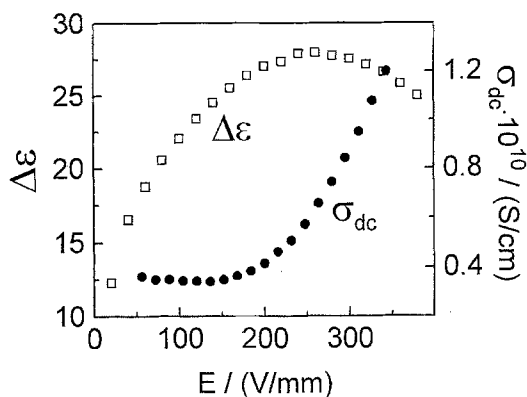


Fig. 2 Dependence of the dielectric relaxation strength $\Delta\epsilon$ and macroscopic conductivity σ_{dc} on electrical field strength E at $T = 60^\circ\text{C}$

course of $\Delta\epsilon(E \geq 250 \text{ V/mm})$, the following experiments were carried out at $E < 250 \text{ V/mm}$, where we can expect $\Delta\epsilon$ to solely reflect structural changes in the ERF.

Since we are in many cases not interested in the absolute amplitudes of the dielectric function or relaxation strength, we normalize the results to the values which designate the data obtained without application of a shear rate or an electrical field, i.e., for $\dot{\gamma} = 0$, $E = 0$. The relaxation strength obtained under these conditions is denoted $\Delta\epsilon_n$ and we define, as discussed previously [12],

$$K_D = \Delta\epsilon / \Delta\epsilon_n. \quad (1)$$

Because the dielectric relaxation time τ_D is not strongly influenced by field or shear rate effects [12], the value of ϵ'' at a particular frequency ω_0 close to the peak position τ_D^{-1} is nearly proportional to $\Delta\epsilon$. We thus use the approximation

$$K_D(t) \approx \epsilon''(\omega_0, t) / \epsilon''(\omega_0), \quad \omega_0 \approx \tau_D^{-1} \quad (2)$$

for time-resolved measurements of $K_D(t)$ which is a faster method compared to recording the entire $\epsilon^*(\omega)$ spectra for delineating $\Delta\epsilon$ [1]. For representative $\epsilon^*(\omega)$ data for this ERF see [12]. The following data have been recorded by monitoring $\epsilon''(\omega_0)$ as a function of time using $\omega_0/2\pi = 1 \text{ kHz}$ or 4 kHz , thereby neglecting the effects due to $\tau_D(E, \dot{\gamma})$ for obtaining $K_D(t)$, which remain small in the present shear rate and field regime. It is also impossible to correct $\epsilon''(\omega_0)$ for the minor contributions arising from the conductivity σ_{dc} , which also does not depend strongly on shear rate and field in the present ranges.

In the same manner we proceed with the mechanical stress $\sigma_M(E, \dot{\gamma}, t)$ where the rheologic analogue to $K_D(t)$ reads

$$K_M(t) = \sigma_M(E, \dot{\gamma}, t) / \sigma_{M,n}(E = 0, \dot{\gamma}, t). \quad (3)$$

The light transmission intensity $I(E, t)$ is normalized according to

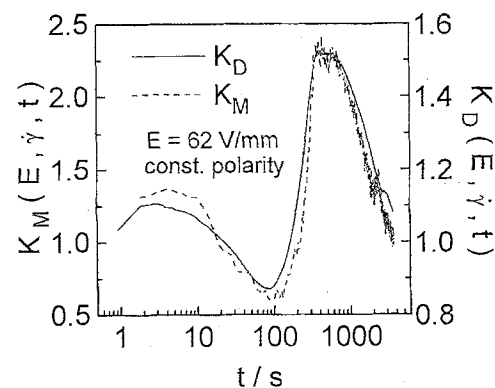
$$K_L(t) = I(E, t) / I_n(E = 0, t). \quad (4)$$

The motivation for focusing on the quantities K_D , K_M and K_L is that the only parameter which affects $\Delta\epsilon(E, \dot{\gamma})$, $\sigma_M(E, \dot{\gamma}, t)$ or $I(E, t)$ at a constant temperature is structural correlation which arises from dipolar particle interactions in the ERF [12]. These structural effects are strongly dependent on electrical field strength E , constant or alternating polarity of the bias field E , application time t_{ON} of E , shear rate $\dot{\gamma}$ and temperature T . $K_D(t)$ and $K_M(t)$ in Fig. 3 show the same time-dependent behavior in the case of identical experimental conditions. This provides evidence for $K_D(t)$ and $K_M(t)$ describing the same phenomena of ERFs in the investigated electrical bias field regime $0 < E < 250 \text{ V/mm}$.

The effect of constant versus alternating polarity (at a rate of 0.75 Hz) of the electrical bias field E is detected in the time range $0.75 \text{ s} < t < 3600 \text{ s}$ as shown in Fig. 4. $K_D(t)$ increases in both types of experiments during the first seconds after switching on a field of $E = 62 \text{ V/mm}$, but after about 10 s $K_D(t)$ decreases if the polarity of the bias field does not alternate periodically. A minimum at $t = 100 \text{ s}$ is detected in this case of constant polarity. For $t > 100 \text{ s}$ $K_D(t)$ increases once more but it becomes not as large as in the case of alternating polarity. The position of the minimum at $t = 100 \text{ s}$ is not dependent on shearing the sample (Fig. 4). The differences between the experiments with ($\dot{\gamma} = 8 \text{ s}^{-1}$) and without shear rate are that the initial response of the ERF at $t \approx 5 \text{ s}$ is smaller and $K_D(t)$ decreases at times $t > 700 \text{ s}$ if a constant shear rate is applied. Figure 5 shows that the position of the minimum shifts towards shorter times with increasing temperature. The differences between the two curves in Fig. 5 at $t > 1000 \text{ s}$ are caused by different shear rates ($\dot{\gamma} = 8 \text{ s}^{-1}$ at $T = 343 \text{ K}$, $\dot{\gamma} = 5 \text{ s}^{-1}$ at $T = 296 \text{ K}$), but as shown in Fig. 4 the shear rate does not influence the position of the minimum.

Light transmission experiments yield the same information concerning the structural ordering phenomena

Fig. 3 Comparison of $K_D(t)$ and $K_M(t)$ in the case of $\dot{\gamma} = 8 \text{ s}^{-1}$ and $E = 62 \text{ V/mm}$ at constant polarity



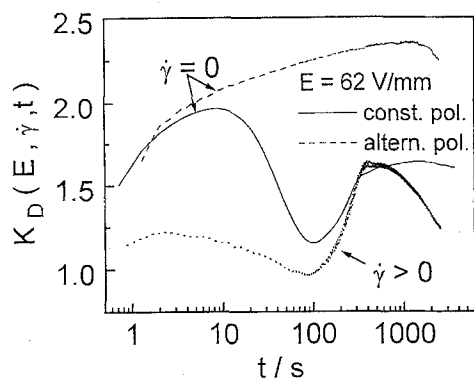


Fig. 4 Dependence of the correlation-factor $K_D(t)$ on polarity switching in the case of $E = 62$ V/mm, $\dot{\gamma} = 0$ and on shearing the sample with $\dot{\gamma} = 8$ s $^{-1}$ for $E = 62$ V/mm at constant polarity

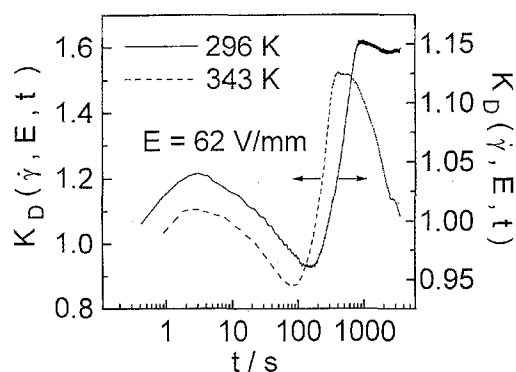


Fig. 5 Dependence of the correlation factor $K_D(t)$ on temperature in the case $\dot{\gamma} = 0$ ($\dot{\gamma} = 8$ s $^{-1}$ at $T = 343$ K, $\dot{\gamma} = 5$ s $^{-1}$ at $T = 296$ K) and $E = 62$ V/mm at constant polarity

described above, since the slopes displayed in the left part of Fig. 6 are the same compared to $K_D(t)$ and $K_M(t)$ in Fig. 3. In addition to the response of $K_L(t)$ to electrical bias fields, the relaxation phenomena after switching off the field are displayed in the right panel of Fig. 6. The effects are completely different for the cases of alternating versus constant polarity of E . After switching off the electrical field with constant polarity K_L decreases and reaches a minimum at $t \approx 4000$ s. It is possible to fit these relaxation phenomena with Eq. (5) with relaxation times $\tau_1 \approx 1500$ s for the decreasing part of $K_L(t)$ and $\tau_2 \approx 10000$ s for the slow increase of $K_L(t)$.

$$K_L(t) = 1 + A_1 \exp(-t/\tau_1) + A_2(1 - \exp(-t/\tau_2)) \quad (5)$$

No minimum is detected in case of alternating electrical bias fields where the ERF relaxes to its initial state (Fig. 6). The relaxation to the initial state takes only ≈ 2000 s compared to nearly 35000 s (Fig. 6) without inverting the polarity of the field. It is not possible to fit the curve in case of constant polarity in the left part of Fig. 6

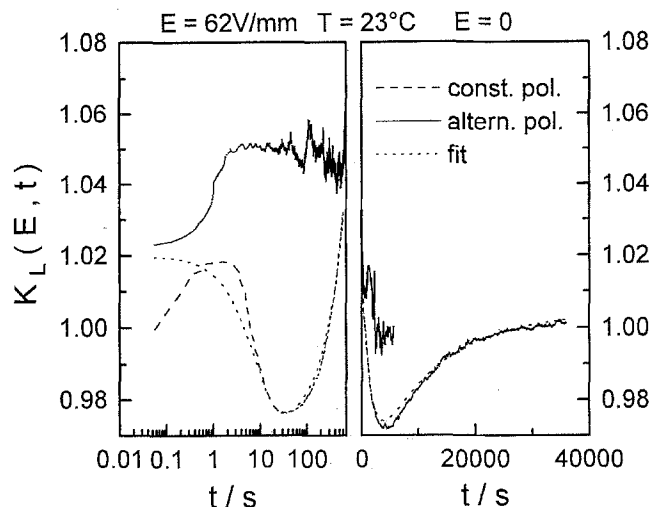


Fig. 6 Left: Dependence of $K_L(t)$ after switching on at $t = 0$ an electrical field $E = 62$ V/mm with constant or alternating polarity. Right: Dependence of $K_L(t)$ after switching off the electrical field. The relaxation times are $\tau_1 \approx 1500$ s and $\tau_2 \approx 10000$ s in the case of constant polarity and $\tau_1 \approx 2000$ s in the case of alternating polarity. The shear rate is $\dot{\gamma} = 0$

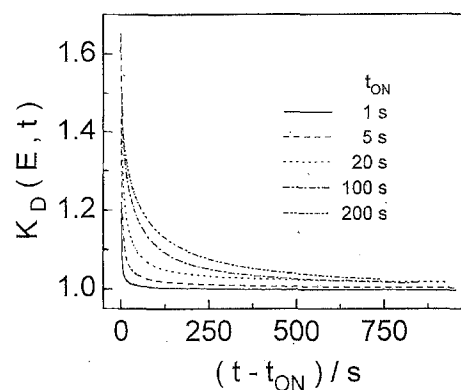


Fig. 7 Dependence of the correlation factor $K_D(t)$ on the application time t_{ON} of a field of $E = 62$ V/mm with switching the field polarity and with a shear rate of $\dot{\gamma} = 0$. t_{ON} is set to 1 s, 5 s, 20 s, 100 s, and 200 s

with the simple Eq. (5), because the decreasing part of the curve is much steeper than the fit.

The relaxation phenomena are not only dependent on constant or alternating polarity of the bias field but also on history. Figure 7 shows the relaxation phenomena when an alternating electrical field (0.75 Hz) that was switched on for a defined application time t_{ON} of 1 s, 5 s, 20 s, 100 s, 200 s, is switched off. After switching off the electrical field the sample needs some time to restore its initial state and the longer the field is applied the larger the relaxation time becomes in the case of no additional shear rate. The case of

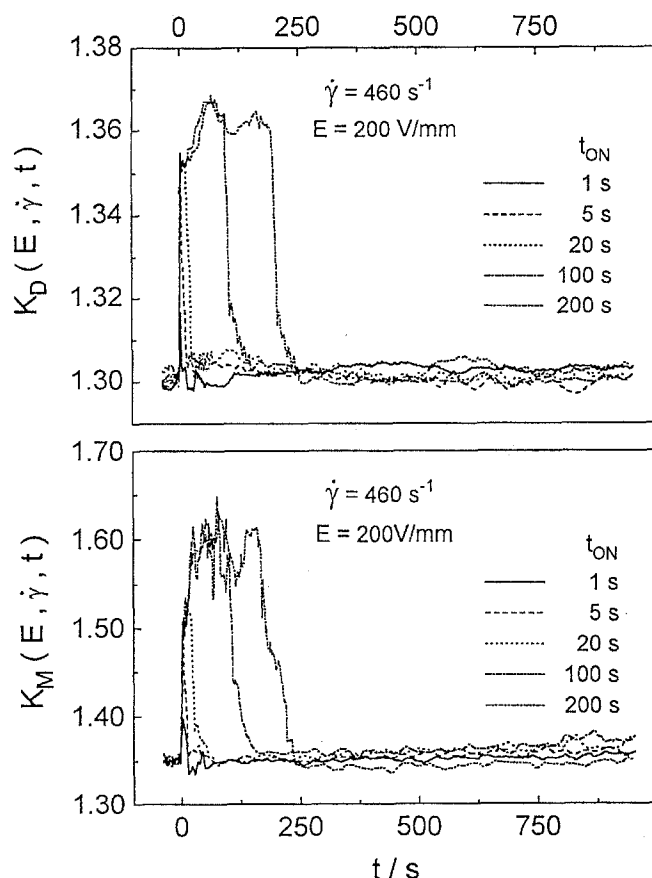


Fig. 8 Dependence of the correlation factors $K_D(t)$ and $K_M(t)$ on the application time t_{ON} of a field of 200 V/mm with switching the field polarity and with a shear rate of $\dot{\gamma} = 460 \text{ s}^{-1}$. t_{ON} is set to 1 s, 5 s, 20 s, 100 s, and 200 s. Rescaling $t \rightarrow t - t_{ON}$ as in Fig. 7 would yield t_{ON} invariant curves which decay faster than the time resolution

simultaneous shearing the ERF during the entire analogous measurement is shown in Fig. 8 for $K_D(t)$ and $K_M(t)$. The relaxation to the initial state of the ERF is faster than without shear rate, but the ΔK is smaller for this case as seen in Fig. 4. Irreversible effects were not found in experiments with an additional shear rate applied to the sample (Fig. 8).

Discussion

In the former section we have introduced the quantities $K_D(t)$, $K_M(t)$ and $K_L(t)$ in a heuristic manner, i.e., we expect for each K to reflect structural effects within the ERF yet without claiming a true linear relation among these quantities. Although the different K 's refer to different experiments, Figs. 3, 6 and 8 readily demonstrate that the appropriately normalized result for $\Delta\epsilon(t)$, $\sigma_M(t)$, and $I(t)$ all trace a common temporal pattern for ~ 3 decades in

time. For the reasons given above we assign the increase in $K(t)$ to the structural ordering which results from applying an electrical field via the strong induced dipole moments of the particles.

In the case of constant polarity of the electrical bias field a maximum of $K_D(t)$ at $t \approx 10 \text{ s}$ and a minimum at $t \approx 100 \text{ s}$ is detected in Fig. 4. Initially ($t < 10 \text{ s}$) the ERF reacts to the electrical field by forming structures [1–4, 13–16], in the same manner as in the case of an alternating bias field. In the case of constant bias polarity at moderate fields electrophoresis occurs, as we have observed directly by optical microscopy. In this situation the particles move to the negative electrical contact because of their net positive charge and the structures formed at short times will be destroyed. This decrease of particle correlations results in a decay of $K_D(t)$ for time $10 \text{ s} \leq t < 100 \text{ s}$ (solid curves in Fig. 4). The dipole-dipole interactions between structurally correlated particles are disturbed by particle motions like that of electrophoresis. When the particles reach the anode of the capacitor new structures are formed and, for this reason, $K_D(t)$ increases once more ($t > 100 \text{ s}$) in the case of constant polarity. The electrophoresis effect at electrical fields smaller than 100 V/mm takes several hundred seconds for a capacitor gap size of about $400 \mu\text{m}$ and can be suppressed by a shear rate $\dot{\gamma} > 0$ as seen in Fig. 4. While the maximum of $K_D(t)$ at $t = 10 \text{ s}$ and the minimum at $t = 100 \text{ s}$ remain at their positions irrespective of the value of $\dot{\gamma}$, $K_D(t)$ decreases for $t > 1000 \text{ s}$ in the case of a sheared sample. Both the decay of $K_D(t)$ at the very long times as well as the less pronounced initial maximum for sheared samples indicate that shear forces counteract structure formation quantified in terms of $K_D(t)$. Additionally, Fig. 5 shows that the effects attributed to electrophoresis are subject to the expected variations with temperature via the viscosity $\eta(T)$ of the silicone oil.

The different response phenomena in the two cases of alternating or constant polarity of the bias field yield different relaxation phenomena when the field is switched off. Figure 6 indicates the response patterns for the optical experiment. The ERF relaxes very slowly to its initial state after switching off the field (right part of Fig. 6) compared to the fast response to applying the field (left part of Fig. 6) if no shear rate is active. $K_L > 1$ is found at $t = 0.1 \text{ s}$ with an alternating polarity of the field because the initial response of the ERF is faster than experimental resolution. For times $t < 0.1 \text{ s}$ the difference seen for the cases of constant and alternating field should not be regarded as significant, since alternating the field is done as slow as 0.75 Hz. The increase of K_L in the range $0 \leq t \leq 1 \text{ s}$ seen in the left part of Fig. 6 is attributed to the formation of chain-like structures, which tend to open new paths for light transmission. These structures formed at $t \leq 1 \text{ s}$

display a long-term stability only in the case of an alternating bias field, which is intended to suppress electrophoresis.

In case of an alternating electrical field the ERF needs ~ 2000 s to relax and in the case of constant polarity it needs more than 35 000 s (right part of Fig. 6). $K_L(t)$ decreases with $\tau_1 \approx 1500$ s and then increases with $\tau_2 \approx 10\,000$ s in the case of constant polarity, but in the other case $K_L(t)$ simply decreases to the initial state. It is possible to correlate structure formation phenomena (right part of Fig. 6) to relaxation features of the ERF after removing the field again (left part of Fig. 6). The slowest response feature (increasing part at $t > 50$ s for $E = 62$ V/mm) is destroyed at first, but is 10 times slower than it arises. These two features are found only in the case of an alternating polarity of the field, so that the second response of the ERF (decreasing $K_L(t)$ at $t > 10$ s) can be assigned to the slowest relaxation. This structure formation, which takes place during the first 50 s, needs several 10 000 s to be destroyed by Brownian particle motion and is attributed to electrophoresis because it is not found in the measurement shown in Fig. 8 in case of an alternating electrical bias field. The observation that the second process after applying a dc-field and the slowest process are not found when using alternating fields indicate that these effects are associated with electrophoresis. A further support for this assignment originates from the obvious feature in Fig. 6, that only the curves related to constant polarity and at times $t \geq 10$ s attain values below $K_L = 1$. The lowered light transmission related to this situation can be regarded as a signature of the onset of electrophoresis, which tends to counteract the slight structure in the idle state due to Coulombic repulsion. Additionally, the effect of strong electrophoresis is not seen at large electrical fields ($E > 1$ kV/mm) [11], but shows a weak temperature-dependence (Fig. 5). The particle's motion becomes slower while the temperature is decreasing, because the temperature varies the viscosity of the silicone oil and therefore the velocity of the particles in case of motion caused by electrostatical forces. Surprising is the fact that the first maximum of $K_D(t)$ is detected at nearly the same position for $T = 23^\circ\text{C}$ and $T = 70^\circ\text{C}$. It was not possible to observe this phenomenon exactly because of the insufficient resolution of the measurement at $t < 5$ s.

The response and the relaxation phenomena of the ERF are strongly influenced by the electrical fields application-time t_{ON} , the time an alternating electrical field is switched on. In the case of large t_{ON} times the particles in the ERF have more time to correlate or to build solid structures. This leads to a weak rising of $K_D(t)$ with time (Fig. 7). The ERF needs much more time to restore its initial state compared to the case of forming structures and

it does not reach its initial state within 1000 s for application times $t_{\text{ON}} \geq 5$ s in the case of no applied shear rate (Fig. 8). We find minor irreversible effects even in the case of regularly alternating electrical fields. The particle dipoles ordered in solid like structures stabilize each other even in the case of no electrical bias field. Only Brownian motion is responsible for the slow decrease of $K(t)$. This effect of the applied electrical bias field can be destroyed by a shear rate so that the ERF relaxes many times faster to its initial state compared to the case without shearing. A disadvantage of additional shearing is that ΔK is smaller, because the shear rate suppresses the structure formation in the ERF. Larger electrical fields are necessary to obtain ΔK values as large as without shearing the sample [11]. The scattering of the measured data in the case of a sheared sample is caused by modulations of $K_D(t)$ and $K_M(t)$ with the frequency of the angular velocity of the rotating cup.

Conclusions

For a commercial ERF we have employed rheodielectric and light transmission measurements to investigate the extent and the dynamics of field induced structuring, which yields the basis for the electrorheological effects. It has been shown that dielectric, mechanical and light transmission experiments reflect the same results concerning particle correlations. The first response of the ERF due to changes in the bias field or shear rate is faster than 1 s, while the following phenomena like electrophoresis are much slower. Electrophoresis of the ERF can be hindered by a shear rate or it can be suppressed completely by periodically alternating the electrical fields polarity. The field-induced structures are stable for more than 100 s in the case of non-sheared samples. An additional shear rate destroys the formed structures many times faster than pure Brownian motion. After application of an alternating electrical field the ERF relaxes faster to its initial state as in case of constant polarity because the particle distribution is not as inhomogeneous as in the case of electrophoresis. The longer the electrical field is applied the longer the ERF needs to relax to its initial state because the particle dipoles stabilize each other even if no electrical field is applied. These observations imply that the effective state of the ERF is dependent on its history and are strongly influenced by experimental conditions like constant or alternating polarity of the electrical field, shear rate or temperature.

Acknowledgement We gratefully acknowledge the support of Bayer AG, Leverkusen, Germany, especially Dr. E. Wendt for placing the samples at our disposal.

References

1. Ginder JM (1993) *Phys Rev E* 47:3418
2. Haas KC (1993) *Phys Rev E* 47:3362
3. Halsey TC (1992) *Science* 258:761
4. Klingenberg DJ, van Swol F, Zukoski CF (1991) *J Chem Phys* 94:6170
5. Adolf D, Garino T, Hance B (1995) *Langmuir* 11:313
6. Anderson RA (1994) *Langmuir* 10:2917
7. Davis LC (1992) *J Appl Phys* 72:1334
8. Tao R, Roy GD (Eds) (1993) *Proceedings of the Third International Conference on Electrorheological Fluids*, World Scientific, Singapore
9. Böttcher CJF (1973) *Theory of Electric Polarization*, Vol 1, Elsevier, Amsterdam; Böttcher CJF, Bordewijk P (1978) *Theory of Electric Polarization*, Vol II, Elsevier, Amsterdam
10. Bloodworth R, Wendt E (1994) *Polymer Preprints* 35:356
11. Bayer AG, Leverkusen (1994) *Provisional product information*, Bayer Silicone
12. Placke P, Richert R, Fischer EW (1995) *Colloid Polym Sci* 273:848
13. Gast AP, Zukoski CF (1989) *Adv Coll and Interf Sci* 30:153
14. Block H, Kelly JP (1988) *J Phys D: Appl Phys* 21:1661
15. Bossis G, et al. (1994) *Europhys Lett* 25:335
16. Adolf D, Garino T (1995) *Langmuir* 11:307